epl A Letters Journal Exploring the Frontiers of Physics

July 2016

EPL, **115** (2016) 14001
doi: 10.1209/0295-5075/115/14001

www.epljournal.org

Sensing dispersive and dissipative forces by an optomechanical cavity

Oren Suchoi and Eyal Buks

Department of Electrical Engineering, Technion - Haifa 32000 Israel

received on 11 July 2016; accepted by B. A. Van Tiggelen on 15 July 2016
published online 28 July 2016

PACS 46.40.-f – Vibrations and mechanical waves
PACS 05.45.-a – Nonlinear dynamics and chaos
PACS 65.40.De – Thermal expansion; thermomechanical effects

Abstract – We experimentally study an optomechanical cavity that is formed between a mechanical resonator, which serves as a movable mirror, and a stationary on-fiber dielectric mirror. A significant change in the behavior of the system is observed when the distance between the fiber's tip and the mechanical resonator is made smaller than about $1\,\mu$m. The combined influence of Casimir force, Coulomb interaction due to trapped charges, and optomechanical coupling is theoretically analyzed. The comparison between experimental results and theory yields a partial agreement.

The study of the interaction between a mechanical resonator and nearby bodies is of great importance for the fields of microelectromechanical systems and scanning probe microscopy. For sufficiently short distances the interaction is expected to be dominated by the Casimir force [1–3], which originates from the dependence of the ground-state energy of the electromagnetic field upon boundary conditions [4–9]. For larger distances, however, other mechanisms such as Coulomb interaction between trapped charges and their image charges [10] and local variations in the work function [11] commonly dominate the interaction.

In this study we investigate the effect of the interaction between nearby bodies on the dynamics of an optomechanical cavity [12–18]. In our setup the optomechanical cavity is formed between two mirrors, a stationary fiber Bragg grating (FBG) mirror and a movable mirror made of aluminum in the shape of a trampoline supported by 4 beams (see fig. 1(a)). The tip of the fiber is blown into a dome shape. Piezoelectric motors are employed for positioning the center of the dome above the center of the trampoline and for controlling the distance d between them. The observed response of the optomechanical cavity in the range $d \lesssim 1\,\mu$m exhibits rich dynamics resulting from the interplay between back-reaction optomechanical effects and the nonlinear coupling between the interacting bodies. In general, such coupling may result in both a static force due to dispersive interaction, and a friction force due to dissipative (or retarded) interaction [19]. Contrary to some other previously employed techniques, in which only the static force can be measured, we find that the observed response of the optomechanical cavity allows the extraction of both static and friction forces [20–22]. The comparison between data and theoretical predictions reveals that some of the experimental findings are not well understood.

A photo-lithography process is used to pattern a 200 nm thick aluminum on a high-resistivity silicon wafer, into a mechanical resonator in the shape of a $100 \times 100\,\mu\text{m}^2$ trampoline [23] (see fig. 1(a)). Details of the fabrication process can be found elsewhere [24]. Measurements are performed at a temperature of 77 K and a pressure well below 5×10^{-5} mbar. A graded index fiber (GIF) having a peak refractive index of $n_{\text{GIF}} = 1.49$ and a pitch of 0.47 is spliced to the end of the single mode fiber (SMF), and its tip is blown into a dome shape of radius $R = 90\,\mu$m. A cryogenic piezoelectric three-axis positioning system having sub-nanometer resolution is employed for manipulating the position of the optical fiber. A tunable laser operating near the Bragg wavelength $\lambda_{\text{B}} = 1545.7$ nm of the FBG together with an external attenuator are employed to excite the optical cavity. The optical power reflected off the cavity is measured by a photodetector (PD), which is connected to both a spectrum analyzer and to an oscilloscope. Two neighboring optical cavity resonances are seen in panel (b) of fig. 1, in which the reflected optical power is plotted as a function of the voltage V_{z} that is applied to the piezoelectric motor, which is

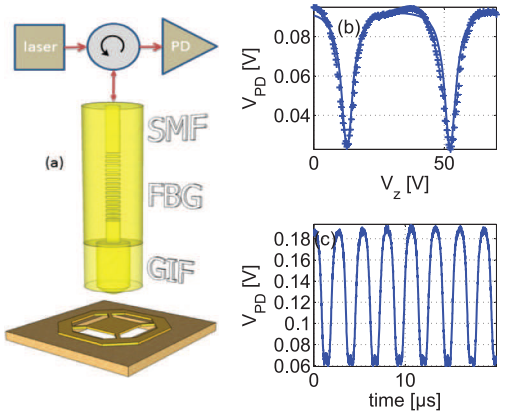

Fig. 1: (Color online) The experimental setup. (a) The fiber probe is composed of a FBG mirror and a GIF lens having a tip that has been blown into a dome shape. A tunable laser excites the cavity and the off-reflected optical power is measured using a photodetector (PD). (b) The PD voltage $V_{\rm PD}$ *vs.* the voltage $V_{\rm z}$ that is applied to the piezoelectric motor controlling the distance between the dome and the trampoline. The crosses represent experimental results, which have been obtained with injected optical power of $P_{\rm L} = 0.90\,{\rm mW}$ at wavelength $\lambda = 1545.525\,{\rm nm}$. The solid line represents the theoretically predicted voltage, which is obtained from the calculated reflection probability $R_{\rm C} = 1 - I(x)/\beta_{\rm F}$, where $I(x)$ is given by eq. (10), with the parameters $\beta_+ = 0.3$ and $\beta_- = 0.15$. (c) The measured PD voltage $V_{\rm PD}$ *vs.* time in the region of SEO with injected optical power of $P_{\rm L} = 1.77\,{\rm mW}$ at the same wavelength.

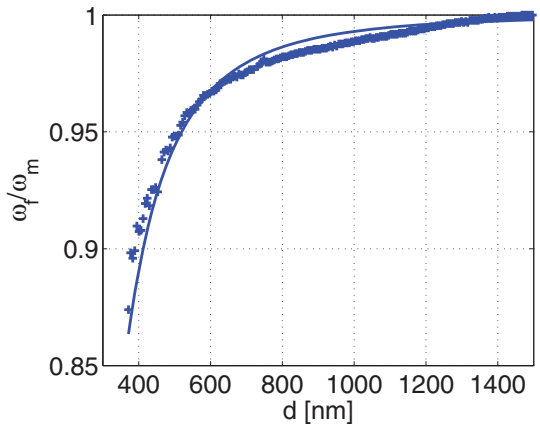

Fig. 2: (Color online) The normalized mechanical resonance frequency $\omega_{\rm f}/\omega_{\rm m}$ *vs.* distance d. The solid line represents the theoretical prediction based on eqs. (1) and (9), whereas experimentally measured values are labelled by crosses. The known value of the effective mass $m = 1.3 \times 10^{-11}\,{\rm kg}$ and the fitting procedure yield the value of trapped charge $q_{\rm T} = 1.5 \times 10^{-14}\,{\rm C}$.

employed for controlling the vertical distance between the dome and the trampoline. A time trace in the region of self-excited oscillation (SEO) is shown in panel (c).

The technique of resonance sensing allows to measure both static and friction forces acting on the trampoline mirror. The linear response of the decoupled fundamental mechanical mode of the trampoline is characterized by a complex angular frequency $\Upsilon_0 = \omega_{\rm m} - i\gamma_{\rm m}$, where $\omega_{\rm m} = 2\pi \times 381.9\,{\rm kHz}$ is the intrinsic angular resonance frequency of the mode and $\gamma_{\rm m} = 1.5\,{\rm Hz}$ is its intrinsic damping rate. In general, interaction between the mechanical mode and a given ancilla system may give rise to an external force acting on the mechanical resonator. For a fixed mechanical displacement x the force is characterized by its static value, which is denoted by $F_{\rm s}(x)$. For simplicity, it is assumed that the time evolution of the ancilla system is governed by a first-order equation of motion, which is characterized by a decay rate $\gamma_{\rm s}$. To lowest nonvanishing order in the coupling strength between the mechanical resonator and the ancilla system the effect of the interaction effectively modifies the value of the complex angular resonance frequency, which becomes $\Upsilon_{\rm eff} = \Upsilon_0 + \Upsilon_{\rm s}$, where the contribution due to the back-reaction $\Upsilon_{\rm s}$ is given by [25]

$$\Upsilon_{\rm s} = \frac{\gamma_{\rm s} F_{\rm s}'\left(x_{\rm f}\right)}{2m\omega_{\rm m}} \frac{1}{\gamma_{\rm s} + i\omega_{\rm m}}\,, \tag{1}$$

where m is the effective mass of the fundamental mechanical mode, $x_{\rm f}$ is the displacement of the mechanical resonator corresponding to a stationary solution of the equations of motion, and it is assumed that $\gamma_{\rm m} \ll \omega_{\rm m}$.

In the discussion below, the contribution to $\Upsilon_{\rm s}$ due to Casimir force is denoted by $\Upsilon_{\rm C} = \omega_{\rm C} - i\gamma_{\rm C}$, the one due to Coulomb interaction induced by trapped charges by $\Upsilon_{\rm T} = \omega_{\rm T} - i\gamma_{\rm T}$, and the one due to optomechanical coupling by $\Upsilon_{\rm B} = \omega_{\rm B} - i\gamma_{\rm B}$. Both contributions $\Upsilon_{\rm C}$ and $\Upsilon_{\rm T}$ become negligibly small when the dome-trampoline distance d is sufficiently large, whereas the contribution of the optomechanical term $\Upsilon_{\rm B}$ can be suppressed by reducing the laser power $P_{\rm L}$.

The normalized mechanical resonance frequency $\omega_{\rm f}/\omega_{\rm m}$ is plotted in fig. 2 as a function of the dome-trampoline distance d. The measured values, which are obtained with laser power of $P_{\rm L} = 0.39\,{\rm mW}$ and laser wavelength of $1545.05\,{\rm nm}$ (the laser is tuned away from the Bragg band of high reflectivity), are labelled by crosses. For these laser parameters optomechanical back-reaction effects are experimentally found to be negligibly small, allowing thus to isolate the combined contributions of $\Upsilon_{\rm C}$ and $\Upsilon_{\rm T}$. To theoretically estimate these contributions, both the Casimir force $F_{\rm C}(d)$ and the Coulomb force due to trapped charges $F_{\rm T}(d)$ are evaluated below as a function of the distance d between the dome and the trampoline.

The Casimir force per unit area $P_{\rm PP}(d)$ between a metal plate having plasma frequency $\omega_{\rm p}$ and a dielectric plate having a relative dielectric constant ϵ separated by a vacuum gap of width d can be evaluated using the Lifshitz formula [5–7,26–28]

$$P_{\rm PP}\left(d\right) = -\frac{3\hbar c\left(\epsilon - 1\right)}{32\pi^2 d^4} I_{\rm L}\left(\frac{d}{d_{\rm p}}, \epsilon - 1\right)\,, \tag{2}$$

where $d_{\rm p} = c/2\omega_{\rm p}$ (6.2 nm for aluminum), the function $I_{\rm L}$ is given by

$$I_{\rm L}(D,y) = \int_1^\infty {\rm d}p \int_0^\infty {\rm d}x \, \frac{x^3}{3p^2 y} \times \left(\frac{1}{\zeta_{{\rm s},1}\zeta_{{\rm s},2}e^x - 1} + \frac{1}{\zeta_{{\rm p},1}\zeta_{{\rm p},2}e^x - 1} \right), \quad (3)$$

where

$$\zeta_{{\rm s},1} = \frac{1 + \sqrt{1 + \left(\frac{D}{x}\right)^2}}{1 - \sqrt{1 + \left(\frac{D}{x}\right)^2}}, \quad (4)$$

$$\zeta_{{\rm p},1} = \frac{1 + \left(\frac{pD}{x}\right)^2 + \sqrt{1 + \left(\frac{D}{x}\right)^2}}{1 + \left(\frac{pD}{x}\right)^2 - \sqrt{1 + \left(\frac{D}{x}\right)^2}}, \quad (5)$$

and where

$$\zeta_{{\rm s},2} = \frac{p + \sqrt{p^2 + y}}{p - \sqrt{p^2 + y}}, \quad (6)$$

$$\zeta_{{\rm p},2} = \frac{(1+y)p + \sqrt{p^2 + y}}{(1+y)p - \sqrt{p^2 + y}}. \quad (7)$$

Note that $I_{\rm L}(D,y) \to 1$ in the limit $D \to \infty$ and $y \to 0$. In eq. (2) the effect of absorption in the dielectric material has been disregarded and the correction due to finite temperature has been neglected. These approximations are expected to be valid provided that $\hbar c/\Delta_{\rm D} \ll d \ll \hbar c/k_{\rm B}T$, where $\Delta_{\rm D}$ is the energy gap of the dielectric material. For the parameters of the current experiment the validity condition reads $22\,{\rm nm} \ll d \ll 30\,\mu{\rm m}$.

When the distance d between the metallic trampoline and the dielectric dome is much smaller than the radius of the dome R the mutual force, which is labeled by $F_{\rm C}(d)$, can be evaluated using the Derjaguin approximation [29] (see eq. (2))

$$F_{\rm C}(d) = 2\pi R \int_d^\infty {\rm d}z \; P_{\rm PP}(z). \quad (8)$$

Finite metal conductivity may give rise to a friction force associated with the Casimir interaction [19]. The effect of Casimir friction on the mechanical resonator can be characterized by a damping rate, which is denoted by $\gamma_{\rm C}$. For the parameters of our device the theoretical expression given in ref. [19] yields a value $\gamma_{\rm C}/\omega_{\rm m} \simeq 10^{-12}$, which is about 7 orders of magnitude smaller than the intrinsic mechanical quality factor, and thus the Casimir friction is not expected to play any significant role in the current experiment [20–22].

Coulomb interaction between trapped charges and their images may give rise to an additional force acting on the mechanical resonator [20]. In general the force depends on the unknown distribution of trapped charges. In what follows, it is assumed that the force can be expressed in terms of an effective total trapped charge $q_{\rm T}$ as [30]

$$F_{\rm T}(d) = \frac{q_{\rm T}^2}{4\pi\epsilon_0 (2d)^2}, \quad (9)$$

where ϵ_0 is the permittivity constant. Note that for the case where all trapped charges are located on the surface of the dome at the point closest to the trampoline eq. (9) becomes exact provided that polarizability can be disregarded. Contrary to the case under discussion in ref. [30], in which the tip is made of a conducting material, in our case the tip (*i.e.*, the optical fiber) is made of an insulating material, and consequently the distribution of trapped charges cannot be controlled by applying a voltage bias to the tip.

In general, trapped charges can give rise to both, a shift in the effective value of the angular frequency of the mechanical resonator, which is denoted by $\omega_{\rm T}$, and to an added damping rate, which is denoted by $\gamma_{\rm T}$. The added damping rate can be evaluated by calculating the damping power generated by dissipative currents on the surface of the metal due to relative motion of trapped charges [31,32]. The ratio $\gamma_{\rm T}/|\omega_{\rm T}|$ is found to be roughly given by $\gamma_{\rm T}/|\omega_{\rm T}| \simeq 4d\omega_{\rm m}/\lambda_{\rm D}\sigma$, where $\lambda_{\rm D}$ is the Debye length ($\simeq 1.7 \times 10^{-10}\,{\rm m}$ for aluminum) and where σ is the conductivity ($\simeq 3.0 \times 10^{18}\,{\rm Hz}$ in CGS units for aluminum at 77 K). For the entire range of values of the distance d that has been explored in the current experiment $\gamma_{\rm T}/|\omega_{\rm T}| < 3 \times 10^{-8}$, and thus the added damping due to trapped charges is expected to be negligibly small. Moreover, retardation in the redistribution of charges on the surface of the metal due to mechanical motion can be safely disregarded since $\sigma \gg \omega_{\rm m}$.

The complex frequency shift $\Upsilon_{\rm C} + \Upsilon_{\rm T}$ induced by the combined effect of Casimir interaction and trapped charges can be evaluated using eq. (1). As was discussed above, the imaginary part of both $\Upsilon_{\rm C}$ and $\Upsilon_{\rm T}$ can be safely disregarded. The fixed point value of the displacement of the mechanical resonator, which is denoted by $x_{\rm f}$, can be found by solving the force balance equation $m\omega_{\rm m}^2 x = F_{\rm C}(d-x) + F_{\rm T}(d-x)$.

As can be seen from fig. 2, the smallest measured value of $\omega_{\rm f}/\omega_{\rm m}$ prior to pull-in is about 0.87. As was previously pointed out in ref. [33], pull-in due to thermal activation (which is estimated to be much more efficient than quantum tunneling for the parameters of the current experiment) is theoretically expected to occur at significantly smaller values of the ratio $\omega_{\rm f}/\omega_{\rm m}$. In the current experiment the pull-in prohibits access to the region of sufficiently small distance d, for which the Casimir contribution to the frequency shift becomes significant, and consequently the theoretically predicted values of $\omega_{\rm f}/\omega_{\rm m}$ (see the solid line in fig. 2) can be calculated to a good approximation by disregarding the contribution due to Casimir interaction. The assumed values of experimental parameters

that have been used in the calculation are listed in the caption of fig. 2.

In the above-discussed measurements back-reaction effects originating from coupling between the optical cavity and the mechanical resonator have been suppressed by keeping the injected optical power P_{L} at a relatively low level. Such effects, however, can significantly modify the dynamics at higher values of P_{L}. In general, the effect of radiation pressure typically governs the optomechanical coupling when the finesse of the optical cavity is sufficiently high [14,16,34–37], whereas, bolometric effects can contribute to the optomechanical coupling when optical absorption by the vibrating mirror is significant [15,38–45], and when the thermal relaxation rate is comparable to the mechanical resonance frequency [43,44,46,47]. Bolometric optomechanical coupling [15,23,25,38,40,46] may result in many intriguing phenomena such as mode cooling and SEO [13,40,43,46,48–56].

In the device under study in the current experiment the dominant underlying mechanism responsible for the optomechanical coupling is optical absorption by the suspended mirror [23]. Such absorption gives rise to heating, which, in turn, causes thermal deformation of the suspended structure due to mismatch between thermal expansion coefficients of the suspended mirror made of aluminum and the supporting silicon substrate [45]. Thermal deformation [40] gives rise to a thermal force, which is expressed as $m\theta T_{\mathrm{R}}$, where θ is assumed to be a constant, and where $T_{\mathrm{R}} = T - T_0$ is the offset between the temperature of the suspended mirror T and the temperature of the supporting substrate T_0. In the static limit the force, which is denoted for this case by F_{B}, can be evaluated by simultaneously solving the force balance equation $\omega_{\mathrm{m}}^2 x = \theta T_{\mathrm{R}}$, where x denotes the mechanical displacement, and the thermal balance equation $Q = \gamma_{\mathrm{H}} T_{\mathrm{R}}$, where Q is the heating power divided by the thermal heat capacity of the trampoline and where γ_{H} is the thermal decay rate.

Optical interference in the cavity gives rise to displacement dependence of the term Q, which is given by $Q = \eta P_{\mathrm{L}} I(x)$, where η is the heating coefficient due to optical absorption and where $P_{\mathrm{L}} I(x)$ is the intra-cavity optical power incident on the suspended mirror. The function $I(x)$ depends on the properties of the optical cavity. The finesse of the optical cavity is limited by loss mechanisms that give rise to optical energy leaking out of the cavity. The main escape routes are through the on-fiber static reflector, through absorption by the metallic mirror, and through radiation. The corresponding transmission probabilities are respectively denoted by $\mathcal{T}_{\mathrm{B}}$, $\mathcal{T}_{\mathrm{A}}$ and $\mathcal{T}_{\mathrm{R}}$. In terms of these parameters, the function $I(x)$ is given by [23]

$$I(x) = \frac{\beta_{\mathrm{F}} \left(1 - \frac{\beta_-^2}{\beta_+^2}\right) \beta_+^2}{1 - \cos\frac{4\pi x_{\mathrm{D}}}{\lambda} + \beta_+^2}, \tag{10}$$

where $x_{\mathrm{D}} = x - x_{\mathrm{R}}$ is the displacement of the mirror relative to a point x_{R}, at which the energy stored in the optical cavity in steady state obtains a local maximum, $\beta_\pm^2 = (\mathcal{T}_{\mathrm{B}} \pm \mathcal{T}_{\mathrm{A}} \pm \mathcal{T}_{\mathrm{R}})^2/8$ and where β_{F} is the cavity finesse. The reflection probability is given in steady state by $R_{\mathrm{C}} = 1 - I(x)/\beta_{\mathrm{F}}$ [23,57].

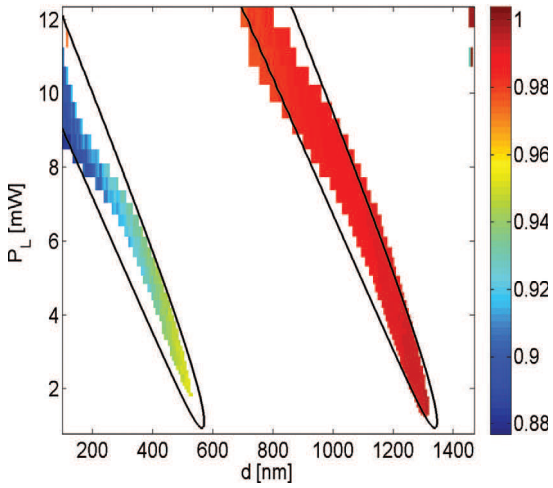

Fig. 3: (Color online) The measured normalized value of SEO frequency $\omega_{\mathrm{SEO}}/\omega_{\mathrm{m}}$ *vs.* dome-trampoline distance d and laser power P_{L}. The black solid lines represent the theoretically calculated bifurcation lines, along which the effective damping rate vanishes. The assumed values of experimental parameters that have been used in the calculation are $\beta_{\mathrm{F}} = 3.0$ and $\omega_{\mathrm{m}}^2 \gamma_{\mathrm{H}} \lambda/\theta\eta = 3.3\,\mathrm{mW}$ (see also the captions of figs. 1 and 2).

With sufficiently high laser power the system can be driven into SEO. The color-coded plot seen in fig. 3 exhibits the measured normalized value of SEO frequency $\omega_{\mathrm{SEO}}/\omega_{\mathrm{m}}$ *vs.* dome-trampoline distance d and laser power P_{L}. No SEO is observed in the white regions. The two colored regions in fig. 3 represent SEO occurring near two optical resonances (OR). The one seen on the left is the first OR of the cavity, which occurs with the smallest value of d, and the one seen on the right is the second one. Note that the excitation frequency (*i.e.*, the laser wavelength) is kept constant and the cavity is tuned by varying the dome-trampoline distance. As can be seen from fig. 3, the SEO frequency ω_{SEO} measured near the first OR is significantly smaller. Moreover, the lowest input laser power value for which SEO occurs near the first OR is significantly higher (the value is 1.45 times larger than the value corresponding to the second OR, which is experimentally found to be similar to other ORs at even larger dome-trampoline distance).

The black solid lines in fig. 3 represent the theoretically calculated bifurcation lines, which are found from solving the equation $\gamma_{\mathrm{m}} + \gamma_{\mathrm{B}} = 0$, where $\gamma_{\mathrm{B}} = -\mathrm{imag}\Upsilon_{\mathrm{B}}$, and Υ_{B}, which is given by eq. (1), is calculated for the case of the above-discussed bolometric coupling between the mechanical resonator and the optical cavity. In spite of the fact that the contribution of both Casimir and Coulomb interactions to the effective mechanical damping rate is theoretically expected to be negligibly small, the experimental results clearly indicate that the damping rate is

significantly larger near the first OR, as can be seen from the significantly higher observed value of the laser power threshold. Note that enhancement in the damping rate is also observed near contact in the low laser power measurements, for which the back-reaction effects are expected to be negligibly small. Further study is needed in order to identify the underlying mechanism responsible for this contactless friction that is observed at relatively short distances.

In summary, sensitive detection of both dispersive and dissipative forces is demonstrated using an optomechanical cavity. The combined effect of Casimir force, Coulomb interaction due to trapped charges and bolometric optomechanical coupling on the mechanical resonator is theoretically estimated. Partial agreement is found in the comparison between theory and experimental findings.

* * *

This work was supported by the Israel Science Foundation, the Binational Science Foundation, the Security Research Foundation at Technion and the Russell Berrie Nanotechnology Institute.

REFERENCES

[1] Lamoreaux S. K., *Phys. Rev. Lett.*, **78** (1997) 5.
[2] Mohideen U. and Roy A., *Phys. Rev. Lett.*, **81** (1998) 4549.
[3] Chan H., Aksyuk V., Kleiman R., Bishop D. and Capasso F., *Phys. Rev. Lett.*, **87** (2001) 211801.
[4] Casimir H. B., *Proc. K. Ned. Akad. Wet.*, **51** (1948) 793.
[5] Lifshitz E., *Sov. Phys.*, **2** (1956) 73.
[6] Milonni P. W., *The Quantum Vacuum* (Academic Press, San Diego) 1994.
[7] Bordag M., Mohideen U. and Mostepanenko V. M., *Phys. Rep.*, **353** (2001) 1.
[8] Lamoreaux S. K., *Am. J. Phys.*, **67** (1999) 850.
[9] Lamoreaux S. K., *Rep. Prog. Phys.*, **68** (2005) 201.
[10] Denk W. and Pohl D. W., *Appl. Phys. Lett.*, **59** (1991) 2171.
[11] Burnham N., Colton R. and Pollock H., *Phys. Rev. Lett.*, **69** (1992) 144.
[12] Braginsky V. and Manukin A., *Sov. Phys. JETP*, **25** (1967) 653.
[13] Hane K. and Suzuki K., *Sens. Actuators A: Phys.*, **51** (1996) 179.
[14] Gigan S., Böhm H. R., Paternostro M., Blaser F., Hertzberg J. B., Schwab K. C., Bauerle D., Aspelmeyer M. and Zeilinger A., *Nature*, **444** (2006) 67.
[15] Metzger C. H. and Karrai K., *Nature*, **432** (2004) 1002.
[16] Kippenberg T. J. and Vahala K. J., *Science*, **321** (2008) 1172.
[17] Favero I., Metzger C., Camerer S., König D., Lorenz H., Kotthaus J. P. and Karrai K., *Appl. Phys. Lett.*, **90** (2007) 104101.
[18] Marquardt F. and Girvin S. M., *Physics*, **2** (2009) 40.
[19] Volokitin A. and Persson B., *J. Phys.: Condens. Matter*, **11** (1999) 345.
[20] Stipe B., Mamin H., Stowe T., Kenny T. and Rugar D., *Phys. Rev. Lett.*, **87** (2001) 096801.
[21] Dorofeyev I., Fuchs H., Wenning G. and Gotsmann B., *Phys. Rev. Lett.*, **83** (1999) 2402.
[22] Gotsmann B. and Fuchs H., *Phys. Rev. Lett.*, **86** (2001) 2597.
[23] Zaitsev S., Pandey A. K., Shtempluck O. and Buks E., *Phys. Rev. E*, **84** (2011) 046605.
[24] Suchoi O., Ella L., Shtempluk O. and Buks E., *Phys. Rev. A*, **90** (2014) 033818.
[25] Zaitsev S., Gottlieb O. and Buks E., *Nonlinear Dyn.*, **69** (2012) 1589.
[26] Chen F., Mohideen U., Klimchitskaya G. and Mostepanenko V., *Phys. Rev. A*, **72** (2005) 020101.
[27] Buhmann S. Y. and Welsch D.-G., *Prog. Quantum Electron.*, **31** (2007) 51.
[28] Bordag M., Klimchitskaya G. L., Mohideen U. and Mostepanenko V. M., *Advances in the Casimir Effect*, Vol. **145** (Oxford University Press, Oxford) 2009.
[29] Derjaguin B. and Abrikosova I., *Sov. Phys. JETP*, **3** (1957) 819.
[30] Marchi F., Dianoux R., Smilde H., Mur P., Comin F. and Chevrier J., *J. Electrostat.*, **66** (2008) 538.
[31] Stowe T., Kenny T., Thomson D. and Rugar D., *Appl. Phys. Lett.*, **75** (1999) 2785.
[32] Chumak A., Milonni P. and Berman G., *Phys. Rev. B*, **70** (2004) 085407.
[33] Buks E. and Roukes M. L., *Europhys. Lett.*, **54** (2001) 220.
[34] Kippenberg T. J., Rokhsari H., Carmon T., Scherer A. and Vahala K. J., *Phys. Rev. Lett.*, **95** (2005) 033901.
[35] Rokhsari H., Kippenberg T., Carmon T. and Vahala K., *Opt. Express*, **13** (2005) 5293.
[36] Arcizet O., Cohadon P. F., Briant T., Pinard M. and Heidmann A., *Nature*, **444** (2006) 71.
[37] Kleckner D. and Bouwmeester D., *Nature*, **444** (2006) 75.
[38] Jourdan G., Comin F. and Chevrier J., *Phys. Rev. Lett.*, **101** (2008) 133904.
[39] Marino F. and Marin F., *Phys. Rev. E*, **83** (2011) 015202.
[40] Metzger C., Ludwig M., Neuenhahn C., Ortlieb A., Favero I., Karrai K. and Marquardt F., *Phys. Rev. Lett.*, **101** (2008) 133903.
[41] Restrepo J., Gabelli J., Ciuti C. and Favero I., *C. R. Phys.*, **12** (2011) 860.
[42] Liberato S. D., Lambert N. and Nori F., arXiv:1011.6295 (2010).
[43] Marquardt F., Harris J. G. E. and Girvin S. M., *Phys. Rev. Lett.*, **96** (2006) 103901.
[44] Paternostro M., Gigan S., Kim M. S., Blaser F., Böhm H. R. and Aspelmeyer M., *New J. Phys.*, **8** (2006) 107.
[45] Yuvaraj D., Kadam M. B., Shtempluck O. and Buks E., *J. Microelectromech. Syst.*, **22** (2013) 430.
[46] Aubin K., Zalalutdinov M., Alan T., Reichenbach R., Rand R., Zehnder A., Parpia J. and Craighead H., *J. Microelectromech. Syst.*, **13** (2004) 1018.

[47] De Liberato S., Lambert N. and Nori F., *Phys. Rev. A*, **83** (2011) 033809.
[48] Kim K. and Lee S., *J. Appl. Phys.*, **91** (2002) 4715.
[49] Carmon T., Rokhsari H., Yang L., Kippenberg T. J. and Vahala K. J., *Phys. Rev. Lett.*, **94** (2005) 223902.
[50] Corbitt T., Ottaway D., Innerhofer E., Pelc J. and Mavalvala N., *Phys. Rev. A*, **74** (2006) 21802.
[51] Carmon T. and Vahala K. J., *Phys. Rev. Lett.*, **98** (2007) 123901.
[52] Bagheri M., Poot M., Li M., Pernice W. P. H. and Tang H. X., *Nat. Nanotechnol.*, **6** (2011) 726.
[53] Rugar D., Mamin H. J. and Guethner P., *Appl. Phys. Lett.*, **55** (1989) 2588.
[54] Arcizet O., Cohadon P.-F., Briant T., Pinard M., Heidmann A., Mackowski J.-M., Michel C., Pinard L., Français O. and Rousseau L., *Phys. Rev. Lett.*, **97** (2006) 133601.
[55] Forstner S., Prams S., Knittel J., van Ooijen E. D., Swaim J. D., Harris G. I., Szorkovszky A., Bowen W. P. and Rubinsztein-Dunlop H., *Phys. Rev. Lett.*, **108** (2012) 120801.
[56] Stapfner S., Ost L., Hunger D., Reichel J., Favero I. and Weig E. M., *Appl. Phys. Lett.*, **102** (2013) 151910.
[57] Yurke B. and Buks E., *J. Lightwave Technol.*, **24** (2006) 5054.